# Magnetic Resonance Imaging Basics

# MR Imaging Revisited

Magnetic Resonance Imaging, commonly known as MRI, is a powerful non-invasive imaging technique. It plays an important role in clinical practices for both diagnosis and pre-surgical planning. Computer based processing and analysis tools have been developed for enhancement, compression, and segmentation of MR images. Development of computer-based visualization and diagnostic tools have enhanced the utility of MR images for different applications. In the present note, we briefly review MR image formation process (MRI physics, & image formation) [HBT99], [HB97]. This note also review currently available techniques and approaches for MR image visualization, processing, and segmentation. This also reviewed MR image based and other diagnostic tools. This examined in more detail's techniques used for processing of MR brain images, which are relevant to our work. However, this note is in no way exhaustive.

# 1. MR Image Formation

Magnetic Resonance Imaging (MRI) is a non-invasive[1] imaging technique used primarily in medical settings to produce images of the inside of the human body. MRI is based on the nuclear magnetic resonance (NMR) phenomenon first observed by Bloch and Purcell in 1946. NMR principles have made high quality image recovery possible by allowing the encoding of spatial information into signals that can be detected outside the body.

The MRI hardware consists of a main magnet along with three gradient coils to provide smaller magnetic fields. The MRI machine is a large cube with a horizontal tube, known as the bore, running through the center (figure 1). The patient lies on his back or stomach so that the part of the body to be scanned is at the isocenter[2] of the main magnet. The main magnet provides a very stable and intense magnetic field while the gradient coils provide variable localized fields. Transmitter coils generate oscillating magnetic fields as probe signals while receiver coils convert magnetic fields into electrical signals.



**Figure 1: A MRI system**

---

[1] Non-Invasive: Not breaking, cutting, or entering skin.
[2] Isocenter: Exact center of the main Magnet.

NMR is based on the principle that any object can be subdivided into atoms. Each atom is composed of two types of charged particles: protons and electrons. Subatomic particles such as electrons and protons have a property known as spin[1]. Although a proper explanation of subatomic particle behavior requires quantum mechanics, MRI principles can be accurately described using classical models because MRI involves collections of particles. Spin is often associated with the angular momentum $\vec{J}$ of the atom and may be visualized as a top spinning about its vertical axis as shown in Figure 2. Spin values come in integer multiples of 0.5 and may be positive or negative. The spin for an unpaired subatomic particle is 0.5. The net spin of a collection of particles is the sum of the individual spins. Techniques based on NMR, including MRI, are dependent on collections of particles with net spin. According to Ampere's law, a time-varying electric charge distribution induces a magnetic field. Consequently, the nucleus of an atom with net spin will produce a small magnetic field. This magnetic field is represented by the vector quantity $\vec{\mu}$ and known as the nuclear magnetic dipole moment or the magnetic moment. The magnetic moment is related to the spin angular momentum by the following relationship:
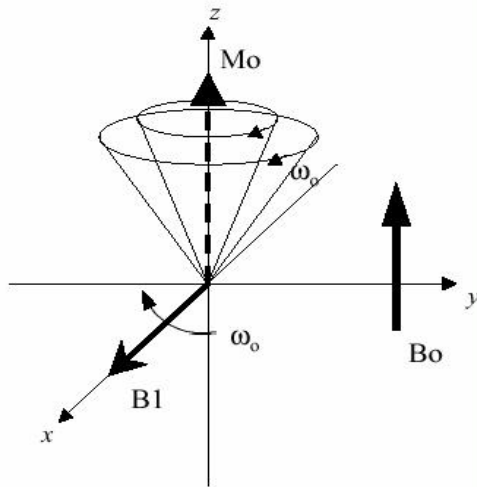
$$\vec{\mu} = \gamma . \vec{j} \qquad (1)$$



**Figure 2: Spin movement in strong magnetic field B$_0$**

---

[1] Spin: Spin is a fundamental property of nature like electrical charge or mass. Spin comes in multiples

The constant of proportionality, $\gamma$, known as the gyromagnetic ratio, is dependent on the nucleus type. The $\gamma$ values for select nuclei are listed in Table (1).

| Nucleus | Spin | Gyromagnetic Ratio |
|---------|------|--------------------|
| 1H      | 0.5  | 42.58              |
| 13C     | 0.5  | 10.71              |
| 19F     | 0.5  | 40.05              |
| 31P     | 0.5  | 11.26              |

**Table 1: NMR properties of some nuclei**

Most clinical applications of MRI require an abundance of hydrogen inside the object to be imaged because its relatively high gyromagnetic ratio eases the imaging process. The human body is primarily fat and water, both of which have many hydrogen atoms. The magnitude of the magnetic moment can be calculated by

$$\mu = \gamma.h.\sqrt{I(I+1)} \tag{2}$$

where $h$ is Planck's constant $h$ (approximately $6.626 \cdot 10^{-34} J \cdot s$) divided by $2\pi$, and I, the nuclear spin quantum number, is the magnitude of the spin value mentioned earlier and must take on a value that is a positive integer multiple of 0.5, such as

$$I = 0, 0.5, 1.0, 1.5, 2.0, 2.5, 3.0 \tag{3}$$

Although the magnitude of $\vec{\mu}$ is known, its direction is random unless an external magnetic field is applied. When placed in an external magnetic field, the magnetic moment vector $\vec{\mu}$ of a subatomic particle will align with the external field in two possible energy states. The low energy

state requires that the magnetic moment align itself parallel to the direction of the magnetic field, as shown in Figure 3. The higher energy state, shown in Figure 3, occurs when the magnetic moment is aligned in the opposite direction as the main magnetic field.
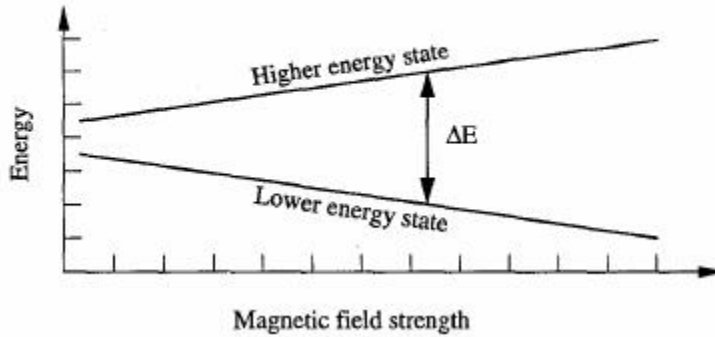


**Figure 3: Low energy and high-energy state of particle**

When placed in a magnetic field of strength B, a particle with a net spin can absorb a photon of frequency $\omega$. The frequency of the absorbable photons is linearly dependent on the strength of the magnetic field:

$$\varpi = \gamma B \tag{4}$$

A particle with net spin can undergo a transition between the two energy states with the absorption of a photon. Because particles have only two discrete energy states, the energy of the absorbed photon must equal the difference between the states. The energy of a photon is linearly dependent on its frequency of the photon:

$$E = h\omega \tag{5}$$

In this case, the constant of proportionality is Planck's constant h. The frequency $\omega$ is known as the Larmor frequency. Equations (4) and (5) can be combined for an expression of the energy between the states:

$$E = h\gamma B \tag{6}$$

In order to create a macroscopic magnetic field inside the body, an external magnetic field is applied. Convention dictates that the field have a strength of $B_0$ and lie along the z-axis such that

$$\vec{B_0} = B_0 \vec{k} \tag{7}$$

where $\vec{i}$, $\vec{j}$, and $\vec{k}$ represent unit vectors in the x, y, and z directions, respectively.

## 2. The Bloch equation

A rotating reference frame is a coordinate system whose transverse (XY) plane is rotating with respect to the laboratory's coordinate system. In this case, the rotation is assumed to be clockwise at a frequency $\omega$. The new axes will be labeled x0, y0, and z0 to distinguish them from the conventional frame. This frame is related to the conventional frame by the following transform:

$$\vec{i'} = \cos(\omega t)\,\vec{i} - \sin(\omega t)\,\vec{j} \tag{8}$$

$$\vec{j'} = \sin(\omega t)\,\vec{i} + \cos(\omega t)\,\vec{j} \tag{9}$$

$$\vec{k'} = \vec{k} \tag{10}$$

The individual spins of the atoms can add up to a bulk magnetization $\vec{M}$ using the following relation:

$$\vec{M} = \sum_{n=1}^{N} \vec{\mu}_n \tag{11}$$

where N is the total number of spins in the object being imaged. At equilibrium, the bulk magnetization vector lies in the direction of the applied uniform magnetic field $\vec{B}_0$ and is represented by $\vec{M}_0$. Conventionally, the uniform magnetic field is applied in the z-direction; therefore, the bulk magnetization vector also lies in the z-direction. There is no transverse ($M_x$ or $M_y$) components for the bulk magnetization, assuming that there are no other external fields other than the main magnetic field. The variations in the bulk magnetization vector can be described by

$$\frac{d\vec{M}}{dt} = \gamma \vec{M} \times \vec{B}_0 \tag{12}$$

Equation (12), known as the simple form of the Bloch equation, describes the precession that the bulk magnetization vector undergoes if the system is left undisturbed.

If the system is perturbed from its equilibrium state, the laws of thermodynamics dictate that it will return to its equilibrium state provided that the perturbing agent is removed and sufficient time is given. If the bulk magnetization has a component in the xy-plane, it will rotate about the z-axis at a frequency equal to the Larmor frequency. This revolution of the bulk magnetization $\vec{M}$ in the xy-plane is known as free precession. The recovery in the axis of the external magnetic field is described by

$$\frac{dM_{z'}}{dt} = -\frac{(M_{z'} - M_{0,z'})}{T_1} \tag{13}$$

where, $T_1$ is the longitudinal or spin-lattice time constant and $M_{z'}$ and $M_{0,x'}$ are the z-components of the instantaneous and equilibrium bulk magnetization vectors respectively. This phenomenon is known as longitudinal relaxation or $T_1$ relaxation. As the bulk magnetization returns to its equilibrium state, the transverse component is attenuated. This decay, known as transverse relaxation or T2 relaxation, is defined by

$$\frac{dM_{x'}}{dt} = -\frac{M_{x'}}{T_2} \qquad (14)$$

where, T2 is known as the transversal or spin-spin time constant and Mx0 denotes the component of the bulk magnetization vector in the x-direction; a similar relationship exists in the y-direction. The two relaxation processes occur simultaneously and are only separated by the axes along which they happen. Experience has shown that $T_2$ is always less than or equal to $T_1$. Unfortunately, equation (14) describes an ideal case. There are two primary factors that contribute to transverse relaxation: molecular interactions and variations in the main magnetic field $B_0$. Molecular interactions contribute to what is known as pure $T_2$ while aberrations in $B_0$ contribute to an inhomogeneous $T_2$ effect. Variations in the main magnetic field change the $T_2$ constant to a $T_2^{(*)}$, related by:

$$\frac{1}{T_2^{(*)}} = \frac{1}{T_2} + \frac{1}{T_{2,in\,hom}} \qquad (15)$$

A general equation describing a change in the magnetization can be obtained by combining the simple Bloch equation with equations (13) and (14):

$$\frac{d\vec{M}_{rot}}{dt} = \gamma \vec{M}_{rot} \times \vec{B}_0 - \frac{(M_{z'} - M_{0,z'})\vec{k'}}{T_1} - \frac{M_{x'}\vec{i'} + M_{y'}\vec{j'}}{T_2} \qquad (16)$$

## 3. Excitation

A uniform external field aligns the individual magnetic moments in the body along the z-axis. The transverse component of the bulk magnetization vector is zero at equilibrium because the magnetic moments have random phases. The phase of a magnetization vector is the angle between the x-axis and the projection of the vector onto the transverse plane. The constituents of the bulk

magnetization vector rotate at the same frequency about the z-axis but are randomly oriented in the transverse plane and cancel each other.

The magnetic moments must constructively interfere or have phase coherence to have a non-zero transverse magnetization component. In order to enforce phase coherence, a perturbing field is added in the transverse plane. Establishment of phase coherence among the processing spins is referred to as resonance. To establish phase coherence, an oscillating magnetic field $\vec{B}(t)$ of the form

$$\vec{B_1}(t) = 2B_1^e(t)\cos(\omega_{rf}t + \varphi)\,\vec{i} \tag{17}$$

is applied in the transverse (xy) plane. The $B_1$ field is also known as an RF pulse because it has a short duration and oscillates in the radio-frequency range. According to Planck's law, the energy associated with an electromagnetic wave is proportional to its frequency:

$$E_{rf} = h\omega_{rf} \tag{18}$$

The energy provided by the RF pulse must equal the difference in the energy states for the magnetic moment. Equation (6) stated that the energy of an absorbed photon is directly proportional to the magnetic field experienced by the atom. Since radiation energy is interchangeable, one can say that the energy for an RF pulse must equal.

$$E = h\gamma B \tag{19}$$

where B is the magnetic field experienced by an atom. If

$$\omega_0 = hB \tag{20}$$

then resonance requires

$$\omega_{rf} = \omega_0 \qquad (21)$$

Equation (21) is known as the resonance condition. When a collection of particles begins to resonate, the bulk magnetization precesses. A group of particles that share the same resonant frequency is called an isochromat. Earlier, it was stated that a time varying electric charge produces a magnetic field; similarly, a time varying magnetic field produces an electric field. This means that any conducting loop resonating at $\omega_0$ can be used as a receiver coil. Specifically, the flux through the resonating external coil by $\vec{M}(r,t)$ can be described by

$$\phi = \int_{object} \vec{B}_r(\vec{r}) \cdot \vec{M}(\vec{r},t) d\vec{r} \qquad (22)$$

where $\vec{B}_r(\vec{r})$ is the laboratory frame magnetic field at location $\vec{r}$. Then, according to Faraday's law of induction, the voltage induced in the coil is

$$v(t) = -\frac{\partial \phi}{\partial t} = -\frac{\partial}{\partial t} \int_{object} \vec{B}_r(\vec{r}) \cdot \vec{M}(\vec{r},t) d\vec{r} \qquad (23)$$

This system is not practical because the output signal represents a sum of all resonant particles and gives no spatial information. Three gradient coils (one for each axis) provide a local change in the magnetic field, thereby changing the resonant frequency and the output signal. For example, a linear gradient field in the z-direction causes the resonant frequency to vary as a function of longitudinal position:

$$\omega = \gamma B = \gamma(B_0 + zG_z) \qquad (24)$$

Therefore, a given RF pulse will only be able to resonate with particles in the transverse plane, orthogonal to the gradient field.

Gradient fields allow the data processing unit to differentiate among slices, but the exact location of a particle is still unknown. One possible solution is to use all three gradient coils simultaneously to isolate a point. However, this is not possible because multiple points can still share the same resonant frequency. Frequency and phase encoding, discussed later, are two mechanisms for encoding spatial information that allow isolation of a point in space in a reasonable amount of time.

## 4. Introduction to Signal Localization

A simple method has been suggested to generate a measurable signal from the subject. A large homogeneous field is applied to uniformly align most of the nuclear spins and an RF pulse is used to establish resonance with those molecules that share the same precession, or Larmor, frequency. This method does not allow the selection of one region of the subject for study; an RF pulse is only frequency selective and all regions sharing the same Larmor frequency are excited in the same manner. If, for example, the doctor would like to see what the problem in the liver is rather than in the heart, he needs to selectively excite the liver area to differentiate between both regions' local magnetic moments of the same material. The methods used to selectively excite regions of the subject and the techniques, which allow distinction among received signal components' origins, are discussed.

There are three methods used in signal localization. The first, slice selection, selectively excites a slice of the subject to image. The slice can be of arbitrary orientation as determined by the gradient coils' direction and relative strength. Once two-dimensional slice is selected, the resultant signal must be processed to determine which part of the slice is sending each component of the signal. The remaining two methods, frequency and phase-encoding are used for this purpose.

## 5. Selective Excitation

Slice selection is the first step in signal localization. In order to allow the RF pulse to be spatially selective rather than only frequency selective, the resonant frequency must be position-dependent. A gradient field produced by the three gradient coils and the shaped RF pulse is required. The gradient coils produce a linearly varying field, which results in resonant frequency varying linearly along the direction of the gradient, or perpendicular to the selected slice, according to

$$\omega(\vec{r}) = \omega_0 + \gamma \vec{G} \cdot \vec{r} \tag{25}$$

where, $\vec{G}$ denotes the gradient and $\vec{r}$, the position. The gradient field is applied during RF excitation in addition to the homogeneous $B_0$ field. The direction of the field remains in the same direction as $B_0$ but the amplitude of the field now varies along the direction of the gradient. Figure 2.4 shows how a slice along the $\vec{G}$ direction is selected with the gradient, $\vec{G}$. The RF pulse is now designed to make use of the slice-selection capability provided by the gradient field. In its general form, an RF pulse is given as: $B_1(t) = B_1^{e}(t)e^{-i\omega_{rf}t}$, where $B_1^{e}(t)$ is the pulse envelope and $\omega_{rf}$ the excitation frequency. The simplest method used to design the RF pulse is the Fourier method. In order to simplify the following expressions, the gradient is assumed to lie in the z-direction and can be written as $\vec{G} = G\vec{k}$, where $\vec{k}$ is the unit vector in the z-direction. The boxcar function in equation (26) can be used to describe the spatial selection of this slice in the x - y plane.

$$p_s(z) = \Pi(\frac{z - z_0}{\Delta z}) \tag{26}$$

The thickness of the slice is given by $\Delta z$ and it is centered at $z = z_0$. As a result of the gradient field, the Larmor frequency at position z is given in equation (25). Like field strength it varies linearly with z-position. The chosen slice can be represented as a boxcar function in frequency as well.

$$p(\omega) = \Pi(\frac{\omega - \omega_0}{\Delta \omega}) \qquad (27)$$

Here $\Delta \omega = \gamma G_z \Delta_z$ is the slice thickness and $\omega_c$ is the frequency at the center of the slice. The Fourier method assumes $B_1(t)$, the RF pulse, is related to p($\omega$), the frequency slice, according to

$$B_1(t) \propto \int_{-\infty}^{\infty} p(\omega) e^{-iwt} df \qquad (28)$$

$$\propto \Delta f \ \text{sinc} \ (pi\Delta ft) e^{-iw_c t} \qquad (29)$$

where, the Fourier transform of the boxcar function is used to obtain the second proportion. Comparing this form with the general RF pulse given above, the excitation frequency, $\omega_{rf}$, is given by $\omega_c$, the frequency at the center of the slice, and the envelope function, $B_1^e(t)$, is given below.

$$B_1^e(t) = A \ \text{sinc} \ (\pi \Delta ft) \qquad (30)$$

A is a constant determined by the flip angle, $\alpha$, according to $\alpha = \int_0^{\tau_p} \gamma B_1^e(t) dt$, where $\tau_p$ is the duration of the RF pulse. The RF pulse will, in practice, differ from equation (28) because it will be definite in duration, lasting only $\tau_p$ seconds, and it will be shifted in time to start at (or after) t = 0. The envelope function of equation (30) can be rewritten to reflect this time shift.

$$B_1^e(t) = A \ \text{sinc} \ [\pi \Delta f(t - \frac{\tau_p}{2})], \qquad 0 < t \le \tau_p \qquad (31)$$

Ignoring pulse truncation effects and assuming the RF pulse is symmetric about $t = \tau_p / 2$, the slice-selection profile of equation (26) can also be rewritten to reflect the effects of a shifted

envelope function. The standard Fourier relationship between a shift in time and resulting phase shift is used.

$$p(z) = \Pi(\frac{z - z_0}{\Delta z})e^{i\gamma G_z (z - z_0)\tau_p / 2} \tag{32}$$

The Bloch equation approach is another, superior method of designing the RF pulse. The linear phase shift $e^{i\gamma G_z (z - z_0)\tau_p / 2}$ introduced across the slice by the slice-selective gradient results in signal-loss due to de-phasing. The constituents of the bulk magnetization vector acquire differing phase shifts according to their position. The phase shift can be removed by applying a refocusing gradient in a process known as post-excitation re-phasing. Using the Fourier method, an acceptable form of the re-phasing gradient can be found. Denoting the re-phasing gradient as Gr,z , the phase at position z during the re-phasing period is given by equation (33). The re-phasing gradient simply adds the same type of phase shift as the slice-encoding gradient.

$$\phi(z,t) = \gamma G_z (z - z_0)\frac{\tau_p}{2} + \gamma G_{r,z}(z - z_0)(t - \tau_p) \tag{33}$$

The phase at the end of a rephasing period of duration $\tau_r$ is

$$\phi(z,t = \tau_p + \tau_r) = \gamma G_z (z - z_0)\frac{\tau_p}{2} + \gamma G_{r,z}(z - z_0)(\tau_r) \tag{34}$$

In order to cancel the phase shifts, $\phi(z,t = \tau_p + \tau_r)$ is set to 0, yielding the following relation between the re-phasing gradient strength and duration.

$$G_{r,z}\tau_r = -\frac{1}{2}G_z\tau_p \tag{35}$$

Therefore, picking either the duration or the strength of the re-phasing gradient will yield the other value. The effectiveness of this method in re-phasing the signal constituents is limited because the de-phasing amount is an approximate value. The actual amount of de-phasing, which occurs

depends on the particular RF pulse and can be more precisely calculated using the Bloch equation. The necessary re-phasing gradient can then be calculated using the method outlined above. In addition to de-phasing due to pulse time shift, pulse truncation should also be considered. Since the RF pulse is limited in time, the actual slice selection will deviate from the boxcar function. This will be further addressed when slice thickness is discussed. Assuming truncation to be a square filter applied to the infinite sinc function of $B_1^e(t)$, the selection profile in frequency is given by a convolution formula:

$$p(\hat{\omega}) = \Pi(\frac{\omega - \omega_c}{\Delta\omega}) * \operatorname{sinc}[\frac{1}{2}(\omega - \omega_c)\tau_p] \tag{36}$$

This formula also neglects the phase shift previously considered.

## 6. Frequency Encoding

Frequency encoding is another method used to excite spins in specific regions. Like the process of slice selection, frequency encoding makes use of the gradient coils and forces the precessional frequency to be a function of spatial location. In contrast, however, this method applies a gradient during signal detection rather than during the RF excitation periods.

An example of frequency encoding in an arbitrary direction, denoted by $\vec{\mu}_{f_e}$, is considered. In addition to the large, homogeneous magnetic field, $\vec{B}_0$, assume there is a linear gradient in the $\vec{\mu}(f_e)$ direction during signal detection. Then the Larmor frequency is given as a function of this direction as follows:

$$\omega(\mu_{\vec{f}e}) = \omega_0 + \gamma \vec{G}_{fe} . \vec{r} \tag{37}$$

where, $\vec{G}_{fe} = (G_x, G_y, G_z)$ is the frequency-encoding gradient in the $\mu_{\vec{fe}}$ direction. This is the same as equation (25) given for slice selection. For an object with spin distribution $\rho(\vec{r})$, the local signal generated by the spins in a volume $d\vec{r}$ about point r is shown in equation (38).

$$dS(\vec{r},t) = \rho(\vec{r})d\vec{r}\, e^{-i\gamma(B_0 + Gfe\cdot\vec{r})} \tag{38}$$

The received signal is the integral of this local signal over the entire object 39.

$$S(t) = \int\limits_{object} dS(\vec{r},t) = \int\limits_{-\infty}^{\infty} \rho(\vec{r})e^{-i\gamma(B_0 + Gfe\cdot\vec{r})t}d\vec{r}$$

$$= ((\int\limits_{-\infty}^{\infty} \rho(\vec{r})e^{-i\gamma(\vec{G}_{fe}\cdot\vec{r})t}d\vec{r})e^{-i\omega_0 t} \tag{39}$$

The signal $e^{-i\omega_0 t}$ can be removed after demodulation. It is important to note that all points along the line $\vec{G}_{fe}\cdot\vec{r} = cons\tan t$ share the same Larmor frequency because they experience the same magnetic field. As shown in Figure 4 these define isofrequency lines perpendicular to the frequency-encoding gradient. The third signal localization scheme, phase encoding, is necessary to distinguish the points along the isofrequency lines.

## 7. Phase Encoding

Phase encoding is the same as frequency encoding except in when the gradient is applied. In phase encoding the auxiliary gradient field is turned on after the slice-selective RF pulse and gradient but prior to signal detection and the frequency-encoding gradient. During the phase-encoding gradient, the object is, in reality, frequency-encoded; however, upon termination of the phase-

encoding gradient, the signals are left with different phases according to their location in the subject. This is illustrated in Figure 5.

Usually the object is linearly phase-encoded in the y-direction, however, an example of the general case of an arbitrarily directed phase-encoding gradient, $\vec{G}_{pe}$, is considered. A gradient, $\vec{G}_{pe} = (G_x, G_y, G_z)$, is applied for a short time, $T_{pe}$, known as the phase-encoding interval, after the RF pulse has been applied. The local signal under the influence of this gradient, in addition to the large, homogeneous field $\vec{B}_0$, is given in equation (40).

$$dS(x,t) = \begin{cases} \rho(x)e^{-i\gamma(B_0\,\vec{k}+\vec{G}_{pe}\cdot\vec{r})t} & 0 \leq t \leq T_{pe} \\ \rho(x)e^{-i\gamma\,\vec{G}_{pe}\cdot\vec{r}\,T_{pe}}\,e^{-i\gamma B_0\,\vec{k}\,t} & T_{pe} \leq t \end{cases} \tag{40}$$

While the gradient is on, $0 \leq t < T_{pe}$, the signal is the same as a frequency-encoded signal. For $t \geq T_{pe}$, however, only the initial phase angle imparted to the signals is present. It is given by $\phi(\vec{r}) = -\gamma\,\vec{G}_{pe}\cdot\vec{r}\,T_{pe}$. The total signal is the integral of the local signal in equation 40 over the entire object:

$$S(t) = \int_{object} dS(\vec{r},t) \tag{41}$$

$$= [\int_{object} \rho(\vec{r})e^{-i\gamma\,\vec{G}_{pe}\cdot\vec{r}\,T_{pe}}\,d\vec{r}]e^{-i\omega_0 t} \tag{42}$$

As in frequency encoding, the carrier signal, $e^{-i\omega_0 t}$, is removed after demodulation.

## 8. An Introduction to k-space

By considering the relationship between spatial encoding and the Fourier transform an alternate representation for encoding, known as k-space, can be arrived at (Figure 4).
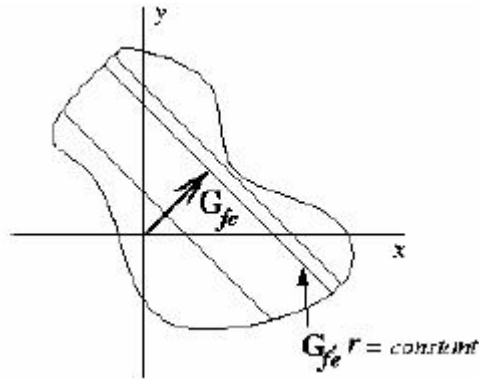


**Figure 4: Frequency encoding space**

By noting that the signal in the last equality of equation (39), after removal of the carrier signals, is a Fourier transform this simpler notation can be used to describe complex sampling and encoding schemes. The Fourier transforms of $\rho(x)$, a general function but in this case the spin density, is given in equation (43).

$$S(\vec{k}) = \int_{bject} \rho(\vec{r}) e^{-i2\pi \, \vec{k} \cdot \vec{r}} \, d\vec{r} \tag{43}$$
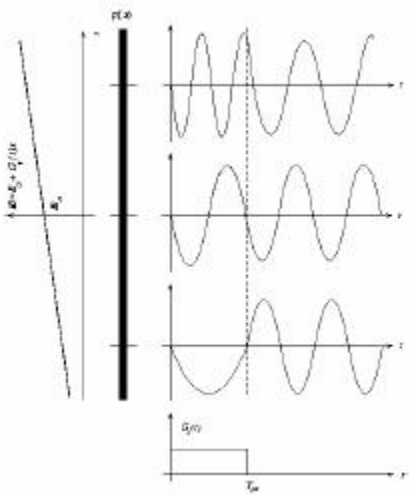


**Figure 5: Phase-encoded signals from a one- dimensional object**

The use of k-space notation in frequency encoding is first considered. Observe that the exponential term in this equation yields the following relation when equated with the exponential term, $-i\gamma(\vec{G}_z \cdot \vec{r})t$, of equation

$$\vec{k} = \begin{cases} \gamma \vec{G}_{fe}\ t & \textit{FID signal} \\ \gamma \vec{G}_{fe}\ (t - T_E) & \textit{Echo Signal} \end{cases} \qquad (44)$$

The gradient provides a mapping from the time domain to k-space. The signal $S(\vec{k})$ exists only for those points in k-space where sampling takes place as defined by the gradient fields. The plot of these points in k-space is called the sampling-trajectory.

As a simple example, consider a constant gradient in the x-direction. In this case, $k_x = \gamma G_x t$, which is seen as a straight line along the kx-axis Figure 2.6a. If the gradient is in both the x and y directions, the line plotted in the kx - ky plane would be at an angle $\phi = \arctan\dfrac{k_y}{k_x} = \arctan\dfrac{G_y}{G_x}$. This is shown in part b of Figure 2.6. Straight lines result only in the case of constant gradients. In the more general case of a time-varying gradient, $\vec{k}$, now a function of time, is given by equation (45).

$$\vec{k} = \gamma \int_0^t \vec{G}\ fe(\tau)d\tau \qquad (45)$$

Phase encoding yields a similar result in k-space. Once again, by comparing the exponent in the Fourier transform of equation (43), with the exponent in the phase encoded signal of equation (41), $-i\gamma(\vec{G}_{pe} \cdot \vec{r})T_{pe}$, a relationship between the gradients and $\vec{k}$ is established. In this case, $\vec{k} = \gamma \vec{G}_{pe}\ T_{pe}$. Since the phase-encoding gradient is applied prior to signal detection, it leaves a constant phase value on each component of the signal according to its location in the object.

Therefore, in phase encoding, $\vec{k}$ has a constant value for a given phase encode interval, $T_{pe}$, and gradient, $G_{pe}$, whereas in frequency encoding, $\vec{k}$ is given as a function of time. This implies phase encoding affects only the starting position of the sampling trajectory in k-space while frequency encoding determines the shape and form of the trajectory. In the more general case of a time varying phase encode gradient $\vec{k}$ is given as

$$\vec{k} = \gamma \int_0^{T_{pe}} \vec{G}_{pe}(\tau)d\tau \tag{46}$$

This is the similar to the expression given in the case of a time varying frequency encoding gradient except it is a constant value. Another important point that can be extracted from equation (46) is that as long as the area under the phase encode gradient remains the same, the starting point of the trajectory will remain the same. The shape of the gradient is inconsequential in this regard. During the phase encode periods, however, $\vec{k}$ varies according to $\dfrac{dk(t)}{dt} = \gamma \vec{G}(t)$ and k moves from the origin to its next trajectory location according to this expression. Therefore, a constant gradient yields a constant speed and a variable gradient, a variable speed.

## 9. Pulse Sequences and the Scanner

A complete example of an MRI scan involving all three-signal localization methods will be considered to clarify the mathematical explanation already given. Figure 7 depicts the setup of the scanner and the orientation of the z-coils. The large, homogeneous field, Bo lies in the z-direction. An image of a slice in the x-y plane is desired. First, using a slice selective gradient in the z-direction, the slice is selectively excited upon application of the tailored RF pulse. The location along the z-axis, which is chosen, varies according to Figure 7; in this example, it is wherever the local field has the same strength as the homogeneous field. It is easily seen, by changing the relative strengths of the auxiliary fields created by the gradient coils in the z-direction the slice

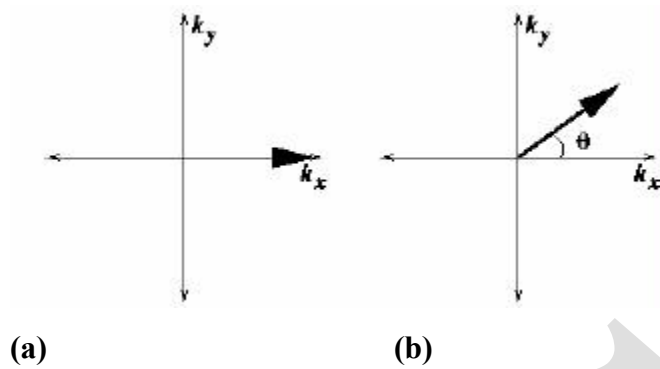moves along the z-axis. As briefly discussed, the RF has finite duration in time, which implies it possesses more than



**(a)**                                    **(b)**

**Figure 6: The sampling trajectories of two simple gradients**
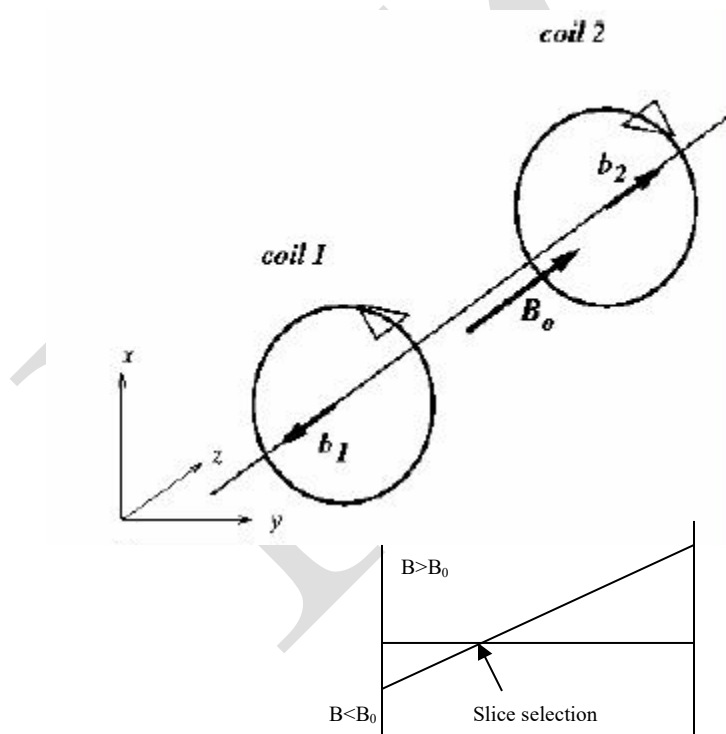


**Figure 7: Slice select gradient coil setup**

one frequency. Since it excites protons precessing at the same frequency, all of those protons sharing the frequencies it possesses will be excited. The bandwidth of the pulse can be changed through varying its duration; the longer it lasts in time the fewer frequencies it will possess. The extreme case being an infinite RF pulse in time possessing a single frequency. As a result of this property, a slice with finite thickness will be selected as protons on either side of $z_0$, the center of the slice, will share similar frequency and be excited by the RF pulse. In practice it is more common to vary the strength of the slice-selective gradient, the magnitude of which determines how rapidly the precessional frequency changes along the z-axis, rather than vary the duration of the RF pulse. Both techniques have the same effect; a large gradient ensures neighboring protons precess at largely different frequencies. Figure 8 illustrates the relationship between slice thickness, RF pulse bandwidth, and gradient strength. Now that the slice has been selected with the simultaneously applied RF pulse and slice-selection gradient, the echo signal emanating from the slice must be further broken down to convey information about regions within the slice. In order to facilitate doing so, the slice is divided into a two-dimensional grid of pixels. In image reconstruction, each pixel is assigned a grayscale value corresponding to the signal strength emanating from its location. Since the slice has a finite width, rather than being two-dimensional areas, the basic units become three-dimensional volumes called voxels[1]. In the example considered here, there will be 256 pixels in the x-direction and 128 pixels in the y-direction, see Figure 9. This means there are 32,768 total pixels or corresponding voxels.
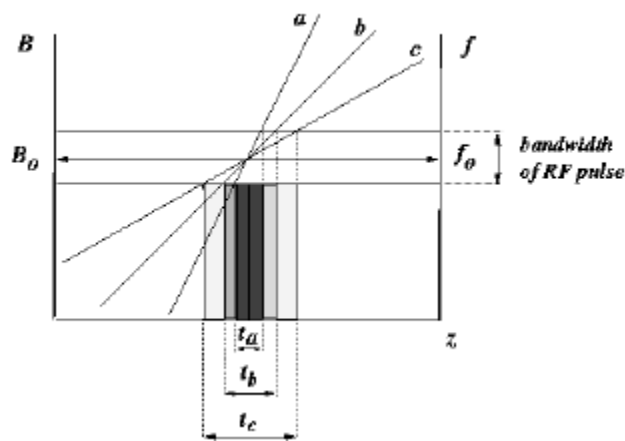


**Figure 8: Relationship between slice thickness and slice thickness gradient**

---

[1] Voxel: **V**oxels are three-dimensional solid, the resolution is frequently different in the three directions.
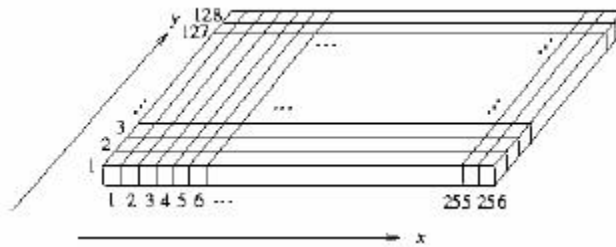
**Figure 9: The selected slice is broken up 256 by 128 grid of voxel**

Frequency and phase encoding will be employed along the x and y-directions, respectively. The x and y gradient coils produce auxiliary fields that vary along their respective directions but whose direction is aligned with the homogeneous field in the z-direction. The coils shown in figure 10.a and 10.b produce the gradients in the x and y directions, or a combination of both. As in slice selection, the relative strengths of the gradient coil fields change the local magnetic field experienced by different locations within the object.
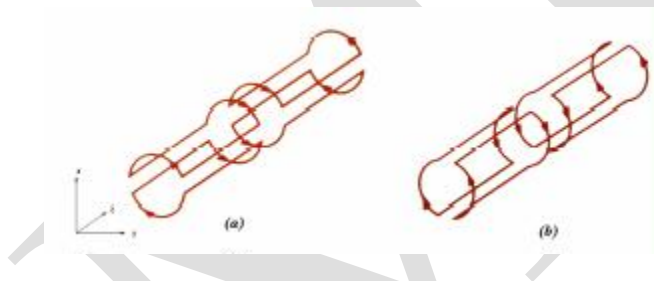


**Figure 10: Shape of Gradients coils: (a) Gradient coil x and (b) Gradient coil Y**

While the echo signal is detected, the frequency encoding gradient, Gx, is applied. Each pixel location along the x-axis will experience a slightly different field and will precess at a corresponding frequency. Those in the same x location, however, will precess at the same frequency yielding the previously discussed isofrequency lines shown in figure 4. A one-dimensional Fourier transform applied to the signal received from the excited slice distinguishes each component according to its frequency or origin along the x-axis. The signal obtained from one x location will be the sum of all 128 pixels along the y-axis that share the same local magnetic

field. Using a one-dimensional Fourier transform and a single MR signal it is impossible to extract position information along the y-direction.

In order to obtain the remaining y-direction information, phase encoding is used. After the slice has been selected, but before frequency encoding and echo detection, a phase-encode gradient is briefly applied in the y-direction. During gradient application each position along the y-direction will experience different local field strength and will precess at the corresponding frequency. After the phase-encode gradient is removed, all positions will resume the same, or nearly the same, precessional frequency, but they will have acquired a different phase. Those having precessed at higher frequency acquiring larger phases and lower frequencies, smaller. Post phase-encode, the phase of the signal will vary linearly according to y-location.

Fourier analysis cannot distinguish the phases of added signals of the same frequency. Therefore, the signals from each x location, which share the same frequency but differ in phase cannot be further decomposed with this technique. However, using phase information and many echos, signal origin in the y-direction can be determined. Each pulse sequence uses a phase-encoding gradient of different strength or duration. Since, in this example, there are 128 locations in the y direction to distinguish, 128 different pulse sequences must be used. The echo signal obtained with each pulse sequence is called a view.

Summarizing, in the x-direction frequency distinguishes the signal origins and in the y-direction the phase given to each of the 128 echos distinguishes them. Each of the 128 resulting echo signals are the samples 256 corresponding to the number of voxels in the x-direction. As will be discussed in the next section, Image Reconstruction, a two-dimensional Fourier Transform of these samples yields the 256 by 128 pixels image. The pulse sequence used in this process is shown in Figure 11. As mentioned in section 1 the echo signal is obtained through the application of the 90 and 180 RF pulses. During these RF pulses, the slice selective gradient in the z-direction is applied.

After the slice is selected, the phase-encode gradient in the y-direction is applied between RF pulses. Finally, the frequency-encoding gradient is applied in the x-direction during echo

detection. The process is repeated for each desired y pixel location, or in this example, 128 times. In the pulse sequence diagram of figure 11 the timing is not to scale; the time between the echo and the 180degree pulse, or echo time, should be a larger percentage than the repetition time, or time between sub subsequent 90degree pulses.

The previous example employs the most basic imaging techniques. Its principles of signal localization, however, can be applied with more complex, superior imaging schemes. These include imaging more than one slice simultaneously, employing three dimensional Fourier analysis on the detected signals, and using ip angles less than 90. Methods such as these improve scanning efficiency and decrease the amount of time the patient is required to be in the scanner.

## 10. Image Reconstruction

The discrete measured data obtained from various sampling methods must be converted into a continuous image function. It is then necessary to digitize this continuous function for computational and display purposes. Figure 3 illustrates this process. Often, discretization is accomplished by performing a FFT on the sufficiently sampled image function.

In this section, basic image reconstruction procedures are discussed. The discretization of the image function, $I(\vec{r})$, is only briefly described. After an overview of the problem, two fundamental reconstruction procedures are described. Finally, a generalized view of all image reconstruction procedures is posed in figure 12.
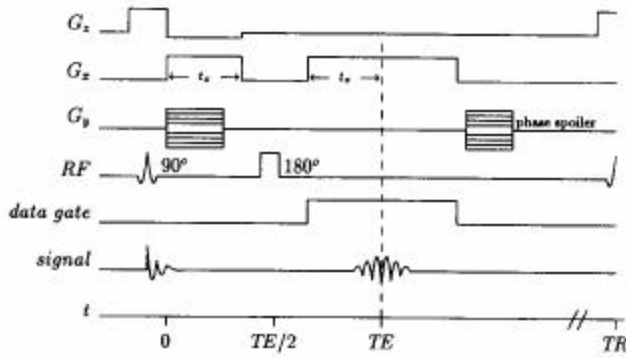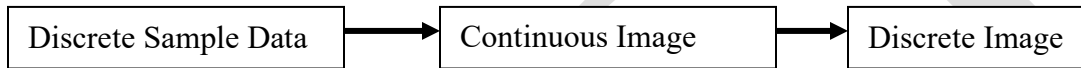
**Figure 11: Spin Echo Pulse sequence**

| Discrete Sample Data | → | Continuous Image | → | Discrete Image |

**Figure 12: Steps of Image reconstruction procedure**

## 11. General Image Reconstruction

Image reconstruction consists of recovering an image function, $I(\cdot)$, which is consistent with the measured k-space data, S, according to:

$$S = T\{I\} \tag{47}$$

where, $T$ in this application is any spatial information encoding scheme, such as the Fourier transform. Any function satisfying equation (47) is called a feasible recon-instruction. Alternatively, $I$ is a feasible reconstruction if any object based on $I$, subject to the same experimental methods, T, yields the same measured data, $S$.

Theoretically, as long as T is invertible an image function can be recovered using the inverse transform:

$$I = T^{-1}\{S\} \qquad\qquad (48)$$

In practice, however, since data space is finite, straightforward computation of $T^{-1}\{S\}$ not possible. Alternate means, such as an approximation to the inverse, are necessary to compute $I$.

Three issues involved with the image reconstruction procedure are existence, unique-ness, and stability. An image function always exists for a given set of measured data since the data are from a physical object. The uniqueness and accuracy of such an image function, however, depends on how data space is sampled and measurement noise. If the sampling is definite, which is always the case in practice, the system is underdetermined and there are many feasible image functions that are consistent with the measured data $S$. Of these, one image function is chosen based on some optimal criteria. Finally, stability relates perturbations in the data, $\Delta S$, to possible error in the reconstructed image, $\Delta I$, where:

$$S + \Delta S = T\{I + \Delta I\} \qquad\qquad (49)$$

Stability analysis of the encoding scheme, T, seeks to evaluate what error in the image, $\Delta I$, is caused by a perturbation in the data, $\Delta S$. The scheme may tend to exaggerate small perturbation in the data resulting in unacceptable error in the reconstructed image. In fact, it can be shown that, in some cases, a negligible error in the data can produce an arbitrarily large error in the image [LL00]. If the operator, or spatial encoding scheme, has this property, as it usually does, and due to finite data sampling, true image reconstruction is actually impossible [LL00]. Sufficient image quality can, however, be obtained by proper selection of the image function and subsequent compensation for known deviations from the true image function.

## 12. Fourier Transform Reconstruction

The most straightforward method of reconstruction uses the Fourier transform in order to recover the image function, $I(\vec{r})$. It is generally used in the case of Cartesian sampling of the data space but, as will be shown later, can be applied to any sampling pattern.

The measured data $S$ are given by

$$S(\vec{k}_n) = \int I(\vec{r}) e^{-i2\pi \vec{k}_n \cdot \vec{r}} d\vec{r}, k_n \in D \tag{50}$$

where, $D$ is the set of k-space samples. In theory, to find $I(\vec{r})$, only the inverse DFT on a set of uniformly spaced samples, S, needs to be computed. As stated before, however, in the case of finite sampling, this is not possible. An alternate computation follows.

The Fourier transform's property of separability is invoked and the evaluation of the inverse considered in one dimension for simplicity. Equation (50) then becomes

$$S(k_n) = \int I(x) e^{-i2\pi k_n x} dx \tag{51}$$

with uniform sampling of k-space, $D = \{k_n n\Delta k, n = ..., -2, -1, 0, 1, 2, ...\}$. Using $k_n = n\Delta k$ equation (51) can be rewritten as

$$S[n] = S(\Delta k) = \int_{-\infty}^{\infty} I(x) e^{-i2\pi n\Delta kx} dx \tag{52}$$

Reconstruction of $I(x)$ can be achieved through use of the Fourier series. Each sample, $S[n]$, may be thought of as a Fourier series coefficient in the following equation derived from the Poisson formula:

$$\sum_{n=-\infty}^{\infty} S[n]e^{i2\pi\Delta kx} = \frac{1}{\Delta k}\sum_{n=-\infty}^{\infty} I(x-n) \tag{53}$$

On the left side, the fundamental frequency of the series is $\Delta k$. The right side is a periodic replication of $I(x)$ with frequency $\Delta k$. There are two cases to consider in evaluating equation (53), one of infinite sampling and the other more practical case of finite sampling. The simpler case of infinite sampling is considered first. Since D, the set of all points in k-space where measurements are taken, ranges from $-\infty$ $to$ $\infty$, the Fourier series in equation (53) is defined. The image function $I(x)$ can be extracted from its periodically extended form if the frequency of its replication satisfies the Nyquist sampling theorem. The image can be reconstructed by picking out any one of its replications as long as $\Delta k < 1/W_x$, where $W_x$ is the support of $I(x)$. The mathematical form of such a selection is:

$$I(x) = \Delta k \prod(\frac{x}{\Delta k})\ \sum S[n]e^{i2\pi\Delta kx} \tag{54}$$

The windowing function, $\prod$, is often omitted for convenience since I(x) is, in practice, only evaluated in this interval. The case of finite sampling is more complex. In this case,

$$D = \{n\Delta k, -N \le n \le N/2\} \tag{55}$$

A unique image function does not exist because $D$ yields a set of data, which is insufficient to define the series in equation (53). Therefore, a feasible image function is not unique. If $I(x)$ is a feasible reconstruction, then $\hat{I}(x) = I(x) + e^{i2\pi m\Delta kx}$ is also a feasible reconstruction for any $|m| > N/2$. In equation (54), $I(x)$ is a feasible reconstruction if the unmeasured coefficients take finite arbitrary values. That is,

$$I(x) = \Delta k \sum_{n=-N/2}^{N/2-1} S[n]e^{i2\pi m\Delta kx}\ +\ \sum_{n<N/2; n\ge N/2} c_n\ e^{i2\pi m\Delta kx} \tag{56}$$

is a feasible reconstruction for arbitrary $c_n$ satisfying $\sum |c_n|^2 < \infty$. The choice of $c_n$ is application-dependent; often, a minimum-norm constraint is used. In this case, the $c_n$'s are chosen to minimize $\int |I|^2 dx$. Application of Parseval's theorem makes all of the unmeasured $c_n$'s then go to zero yielding the following truncated Fourier series known as the Fourier reconstruction formula:

$$I(x) = \Delta k \sum_{n=-N/2}^{N/2-1} S[n] e^{i2\pi\Delta kx}, |x| < \frac{1}{\Delta k} \qquad (57)$$

Truncation causes ringing artifacts in the reconstructed image. In order to minimize ringing, a windowing function, $w_n$, is usually applied to the data samples to smooth the decay at $n = \pm N/2$. However, the image function will no longer produce the same measured data, $S[n]$, when the spatial encoding operator, $T$, is applied to it. Rather, it produces $w_n S[n]$. The known deviation caused by the windowing function is then compensated for in the image.

At this point, assuming the continuous reconstructed image function, $I(x)$, is available, it needs to be digitized for computation and display. As stated earlier, this will not be covered in depth. In short, a DFT is applied to $I(x)$; usually this is accomplished via the FFT in order to improve computational efficiency.

## Publications:

[HBT99]    Haacke EM, Brown RW and Thompson MR Venkatsan R. "Magnetic Resonance Imaging: Physical Principles and sequence Design". J. Wiley and sons, NY, ISBN: 0471-35128-8 1999.

[HB97]    Hashemi RH and Bradley Jr. WG. "MRI: The Basic, Lippincott, Williams and Wilkins, Baltimore", ISBN: 0-6831-8240-4,1997.

[LL00]    Liang, ZP. Lauterbur PC (2000), "Principles of Magnetic Resonance Imaging". IEEE Press, New York.